Fermi National Accelerator Laboratory

FN-371
2562.000
CDF Note No. 134
September 8, 1982

GAS SAMPLING CALORIMETER STUDIES IN PROPORTIONAL, SATURATED AVALANCHE, AND STREAMER MODES

M. Atac, F. Bedeschi, and J. Yoh

Fermi National Accelerator Laboratory
Batavia, Illinois 60510

R. Morse and M. Procario

University of Wisconsin
Madison, Wisconsin 53706

Introduction

Recently, satisfactory new results were obtained at SLAC from gas sampling calorimeters running in the saturated avalanche mode[1] within the energy range of 1.5 to 17.5 GeV. To study the higher energy behavior of this mode, more tests were carried out in the M4 beamline at Fermilab. This paper contains results obtained from the MAC prototype electromagnetic and hadronic calorimeters running in the proportional, saturated avalanche, and the streamer[2] regions for energies between 12 and 150 GeV.

Gas sampling calorimeters have gained in popularity during the last few years because of needs for fine granularity especially in colliding beam experiments at superhigh energies in order to provide a detector with good pattern recognition capability and e, γ, π, and μ identification within dense tracks. This can be achieved by providing sufficiently small cathode pads, strips which are grouped longitudinally in two or three sections.

The main goal of this work has been to study energy resolution and linearity as a function of chamber gain and particle energy. As we will see from the data presented in this paper, that there is a substantial improvement in the energy

resolution as the chamber gain approaches the saturated avalanche region. The resolution is still good in the streamer region with the hadron calorimeter for energies, although only around 25 GeV and below.

Sufficiently large signals obtainable in the saturated avalanche mode eliminate needs for preamplifier, simplifies electronics construction and calibration, and reduces cost.

Description of the Calorimeters

The calorimeters studied were the two MAC prototypes,[3] a hadron, and an electromagnetic calorimeter. We will not describe the electromagnetic calorimeter here since it is fully described in Reference 1 and 3.

Fig. 1 shows the arrangement of the hadron calorimeter. It is composed of 35 chamber planes and 35 iron plates of 2.7 cm thick, a total of 5.7 absorption lengths. The details of the wire plane are given in the figure. The whole assembly, including the distributed storage capacitors, was placed in an aluminum container that could be evacuated for fast flushing with 49.3 percent argon, 49.3 percent ethane, and 1.4 percent ethyl alcohol mixture which was the detector gas during the entire tests. As shown in the figure, the anode wires of each plane were connected to a common strip, and odd and even planes were grouped together for studying 2.7 cm and 5.4 cm thick iron sampling. 60 meter long RG58/U coaxial cables carried the total charge obtained from these groups to two channels of LeCroy 2249W ADC's which were gated with 2.5 μsec wide pulses. The wide gate width was due to very large grouping of wires whose capacitance exceeded 12 nF that caused long decay times. There was no need for amplifiers between the wires and the ADC.

Indeed, it was necessary to attenuate the large signals from the large group of wires with attenuators valued between 2 db and 58 db (in the streamer mode) depending on the high voltage. The gas pressure was kept around atmospheric pressures at all times. The detector gas was replenished every two or three weeks.

M4 Beamline

Fig. 2 shows the essential part of the layout. The M4 beamline was made to provide charged secondaries up to 200 GeV/c with emphasis on high momenta particles. A sweeper dipole and a 3 mm thick lead converter were added upstream to produce a clean electron beam by sweeping out the charged particles and converting γ's from the π^0 decay. Indeed, this was very successful as it will be shown later. Electron contamination of the hadron beam energies above 35 GeV was 2-3 percent. This contamination was eliminated by using a 10 cm thick lead brick upstream.

The particles in the beam were momentum analyzed by a spectrometer consisting of four EPB dipole magnets and three (x,y) sets of multiwire proportional chambers with 1 mm spacing which provided momentum determination accuracy of $\Delta p/p \lesssim 0.5$ percent at high beam momentum. At lower momentum, the multiple scattering, due to scintillators, chambers, and several meters of air gap, causes a significant deterioration in momentum determination. This was monitored by the chambers measuring beam broadening in the nonbend vertical plane which was determined to be $\Delta p/p \simeq 32$ percent/p (GeV).

The trigger was SC1 · SC2 · SC3 · $\bar{V}$ between SC1, SC2, and SC3 scintillation counters, and the whole veto was used for eliminating events containing particles away from the defined part of the beam. A pile-up gate was used in the trigger to reject tracks too closely following each other.

Hadron Calorimeter Results

σ_{rms} values of total pulse height distributions were obtained from Gaussian fits to the data. Only that portion within $\pm 1.5\sigma$ of the mean were used in the fitting procedure. The resolution of the calorimeter to various energies of negatively charged hadrons is shown in Fig. 3. Energy resolution σ/E is linearly dependent on $E^{-1/2}$ with a dependence of $\sim$ 73 percent/$\sqrt{E}$ up to the momenta around 50 GeV/c, and it gets worse beyond that. This may be clarified as we look at the following results.

The σ/E dependence on high voltage (i.e. gas gain) and particle energy was studied. Fig. 4 shows that the resolution is substantially better as the gain increases owing to less fluctuations in the total pulse heights. We believe this is due to gain suppression for highly ionizing tracks. More soft particles are produced in hadronic cascades than purely electromagnetic cascades; therefore, this should be more pronounced in the hadronic case. The improvement in resolution continues well into the self quenching streamer region for 25 GeV. An earlier work[2] showed that some streamer transition starts around 2.6 kV and reaches its full transition above 2.85 kV. σ/E appears to get worse around full transition. This can be attributed to the fact that the cell size of 1.7 cm is too wide, and a large fraction of the tracks may not make streamers due to the space charge saturation in dense tracks. This gets worse at 50 and 75 GeV as seen in the figure.

Experiments were performed to measure the magnitudes of saturation in the saturated avalanche region. For this study, the gain characteristics of an electromagnetic calorimeter tube (9.5 mm x 9.5 mm) was measured as a function of the high voltage for x-rays of 1.5, 3, 5.9, 8, and 22 keV. The results are shown in Figs. 5 and 6. The gain suppressions are clearly demonstrated in Fig. 6, the larger the x-ray energy, the larger the suppression.

Fig. 7 shows the total charge obtained from the calorimeter at various high voltage settings for 25 GeV hadrons. The gain suppression effect for highly ionizing soft tracks is clearly seen, although the calorimeter response is perfectly linear for energies up to 50 GeV and high voltage values up to 2.6 kV as shown in Figs. 8a, b, and c. Around 75 GeV and above, there is some departure from linear response. At 100 GeV, 3 percent of the total charge is lost due to the energy leakage, and the rest of the deviation may be due to the space charge saturation for the dense tracks.

The total charge distribution for 50 GeV hadrons seen in Fig. 9a is reasonably good Gaussian with a slight asymmetry on the lower energy side. This is more clearly seen with the logarithmic plot, Fig. 9b. Figs. 10a and b show that the asymmetry gets larger at 75 GeV. This lower energy part was compared with the data[4] obtained from a comparable absorption length of a calorimeter composed of scintillator iron sampling type. Fig. 11 shows the same type of asymmetry which is due to the energy leakage.

σ/E was studied for 5.4 cm thick sampling by looking at the response from the odd or even chamber sum. They were very identical in response. Fig. 12 shows σ/E versus $E^{-1/2}$ for thick sampling. It is interestingly $\sqrt{2}$ times the σ/E values obtained for 2.7 cm sampling.

Large and clean muon signals were detected through the calorimeter. Fig. 13a shows two peaks. The lower one is the composition of the pedestal and the muon peaks. The higher peak is the distribution for the 75 GeV hadrons. Fig. 13b shows the expanded view of the composite peak. In this picture, the pedestal distribution and the μ-peak are clearly seen. σ_{rms} of the pedestal is less than one count, and the μ-peak corresponds to 2.2 GeV determined from the π^-/μ^- pulse heights shown in Fig. 14. The ratio is quite flat within the error.

The self quenching streamer regime was investigated while the calorimeter was fully efficient to the streamer transition at 3 kV. Fig. 15 shows the total charge as a function of the hadron energy. Large space charge saturation is showing its effect, thus the σ/E stays constant above 25 GeV as seen in Fig. 16.

Electromagnetic Calorimeter

The electron beam was quite clean in the way it was produced as mentioned earlier. Momentum uncorrected on-line histogram data for 17 GeV electrons as shown in Fig. 17 indicate this cleanliness. σ_{rms} of the pedestal distribution is less than one count.

Fig. 18 shows that σ/E gets appreciably better as the gain approaches the saturated avalanche regime for 17 GeV electrons. Then it gets worse as the space charge limitation begins due to dense tracks at higher gains. One way to improve this is to use smaller size tubes and more heavily quenching gases.

Multiple scattering corrected energy resolution, σ/E of the calorimeter as a function of $E^{-1/2}$ is shown in Fig. 19. It is remarkably good up to 100 GeV extrapolating to the origin.

Total pulse height as a function of energy (Fig. 20) shows that linearity is good up to 40 GeV; beyond that it deviates from the linear behavior due to the space charge saturation as mentioned earlier.

Conclusions

The deviation from linearity above 50 GeV makes the σ/E get worse in the saturated avalanche region and beyond. We believe that this is due to the space charge saturation per wire for very high track densities. One way to improve this is to reduce the cell size. 17 mm wide cell of the hadron calorimeter is rather large.

The linearity can be improved at the expense of σ/E by lowering the high voltage. An optimum voltage may be found depending on the energy regime of interest.

Acknowledgments

The authors express their appreciation to R. Coombes, R. Preepost, and D. Ritson for providing the prototype calorimeters; to W. Chinowsky, P. Constanta, J. Freeman, P. McIntyre, R. Loveless, and G. Panorakis for their help in data taking; to M. Hrycyk and J. Urish for setting up the experiment; and to the Meson Laboratory staff for their support.

References

Ref. 1 M. Atac et al., AIP Conference Proceedings No. 3, Particles and Fields Subseries No. 26, 284 (1981); and to be published in Nucl. Instr. and Meth.

Ref. 2 M. Atac et al., Fermilab Report FN-337 (1981) and IEEE Trans. on Nucl. Sci., Vol. NS-29, No. 1, 388 (1982), and to be published in Nucl. Instr. and Meth.

Ref. 3 R. L. Anderson et al., IEEE Trans. on Nucl. Sci., Vol. NS-25, 340 (1978).

Ref. 4 F. Scuilli, Columbia University, private communication.

Figure Captions

Fig. 1 Experimental arrangement.

Fig. 2 Essential part of the M4 beam layout.

Fig. 3 Hadron calorimeter resolution, σ/E, versus $E^{-1/2}$.

Fig. 4 σ/E dependence on high voltage for the hadron calorimeter.

Fig. 5 Gain versus high voltage for various x-ray energies using 9.5 mm x 9.5 mm tube which is a replica of the electromagnetic calorimeter. Clear saturations are seen in the saturated avalanche region.

Fig. 6 Pulse height versus x-ray energy showing large deviations from the linear behavior in the saturated avalanche region.

Fig. 7 The total pulse height versus high voltage obtained from the hadron calorimeter for 25 GeV.

Fig. 8a, b, c Pulse height versus energy for high voltage settings of 2.2, 2.5, and 2.6 kV for the hadron calorimeter.

Fig. 9a and b The total charge distribution for 50 GeV hadrons. The low energy tail which is due to energy leakage is more clear with log-plot as shown in Fig. 9b.

Fig. 13a and b — On-line pulse height distributions obtained from the hadron calorimeter at 75 GeV. Fig. 13a shows the hadron peak and the composite peak of the pedestal and the muon distributions. Fig. 13b is the expanded view of the composite peak. The μ and the pedestal distributions are cleanly separated.

Fig. 14 — π^-/μ^- pulse heights ratio as a function of the high voltage. It is consistent with a constant behavior.

Fig. 15 — The total pulse height distribution obtained in the streamer region as a function of hadron energy showing large deviations due to space charge saturation.

Fig. 16 — σ/E versus $E^{-1/2}$ in the streamer mode.

Fig. 17 — On-line pulse height distribution for 17 GeV obtained from the electromagnetic calorimeter. It shows that the electron beam was very clean. The pedestal distribution is also shown.

Fig. 18 — σ/E versus high voltage for the electromagnetic calorimeter at 17 GeV.

Fig. 19 — σ/E versus $E^{-1/2}$ for the electromagnetic calorimeter.

Fig. 20 — Total pulse height versus energy showing some departure from linearity above 35 GeV for the electromagnetic calorimeter.

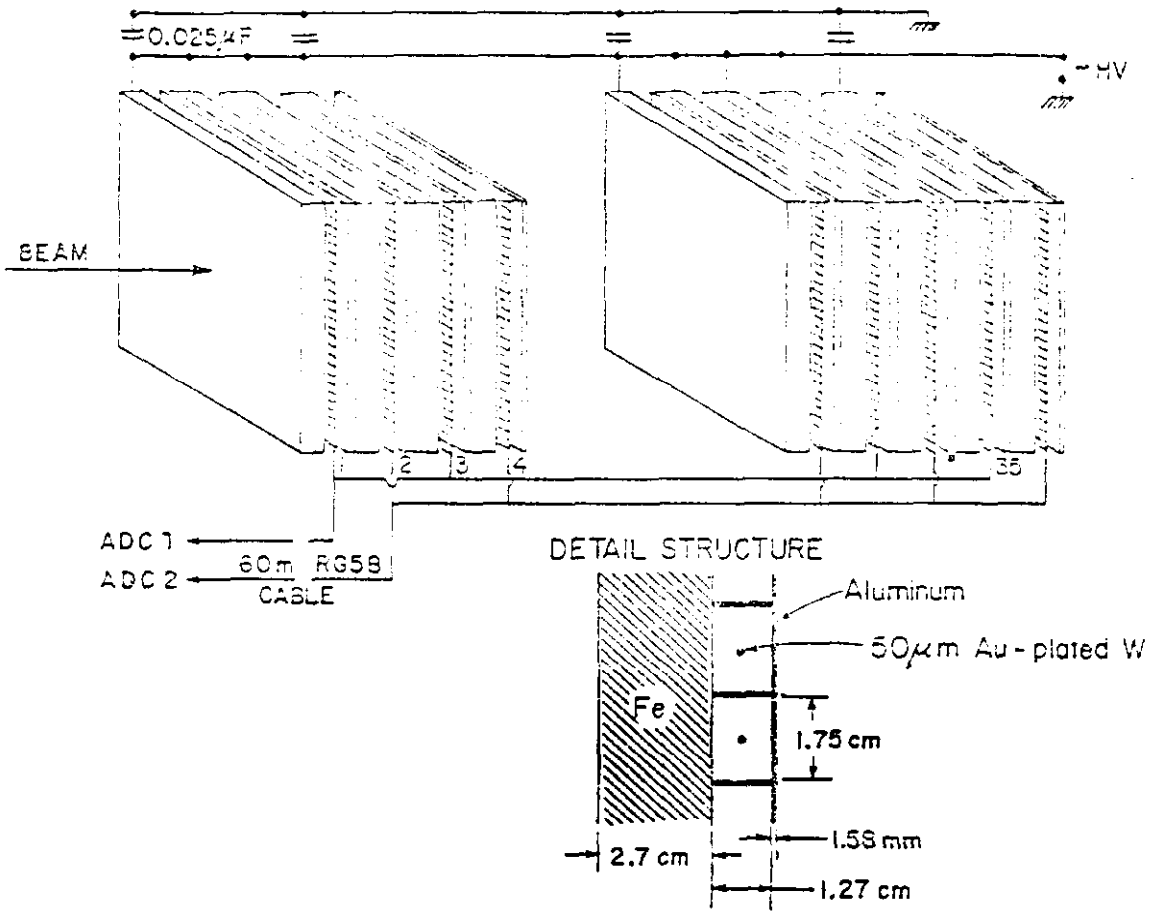
0.025μF
-HV
BEAM
1
2
3
4
35
ADC 1
ADC 2
60m RG58
CABLE
DETAIL STRUCTURE
Aluminum
50μm Au-plated W
Fe
1.75 cm
1.58 mm
2.7 cm
1.27 cm

Fig. 1

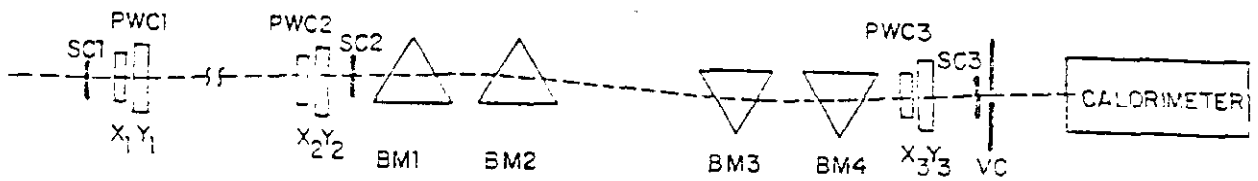
PWC1
SC1
X1 Y1
PWC2
SC2
X2 Y2
BM1
BM2
PWC3
SC3
BM3
BM4
X3 Y3
VC
CALORIMETER

Fig. 2

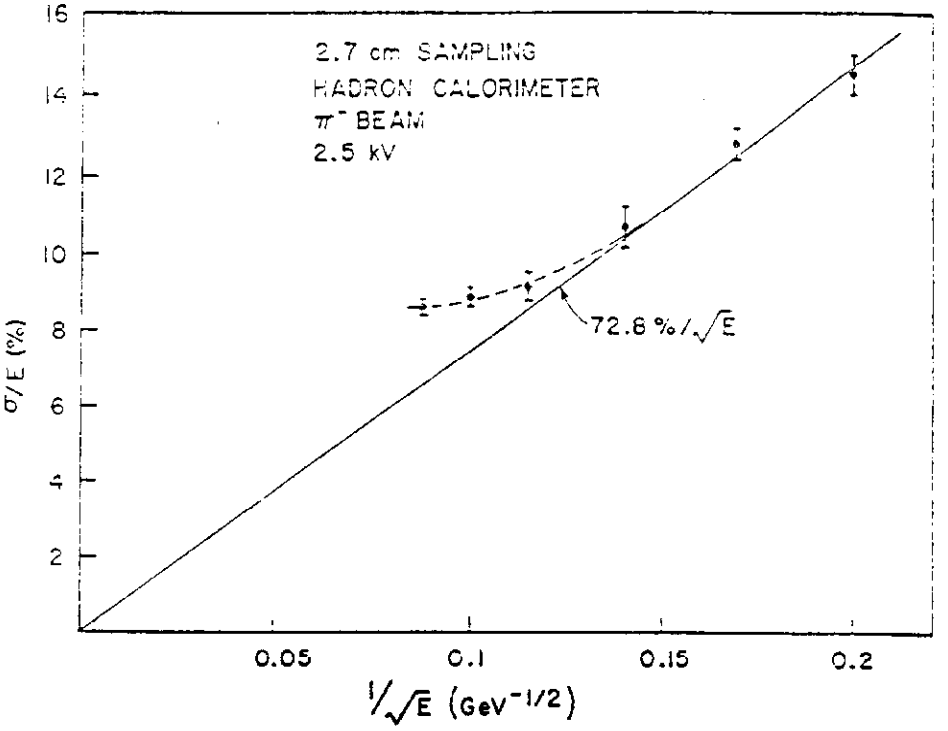
2.7 cm SAMPLING
HADRON CALORIMETER
π⁻ BEAM
2.5 kV
72.6 %/√E
σ/E (%)
1/√E (GeV^-1/2)
16
14
12
10
8
6
4
2
0.05
0.1
0.15
0.2

Fig. 3

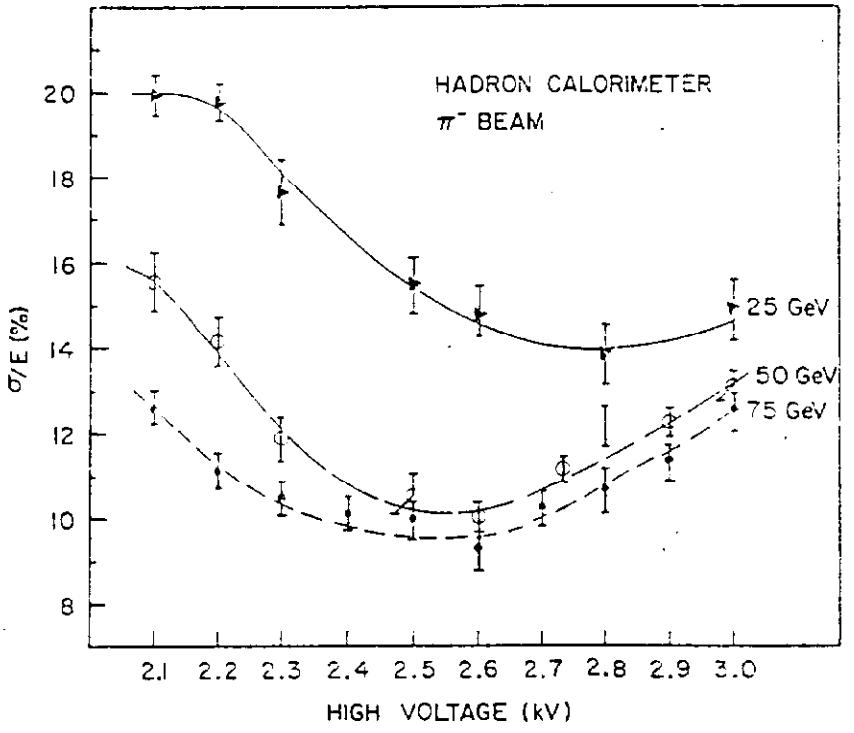
HADRON CALORIMETER
π⁻ BEAM
25 GeV
50 GeV
75 GeV
σ/E (%)
HIGH VOLTAGE (kV)
20
18
16
14
12
10
8
2.1
2.2
2.3
2.4
2.5
2.6
2.7
2.8
2.9
3.0

Fig. 4

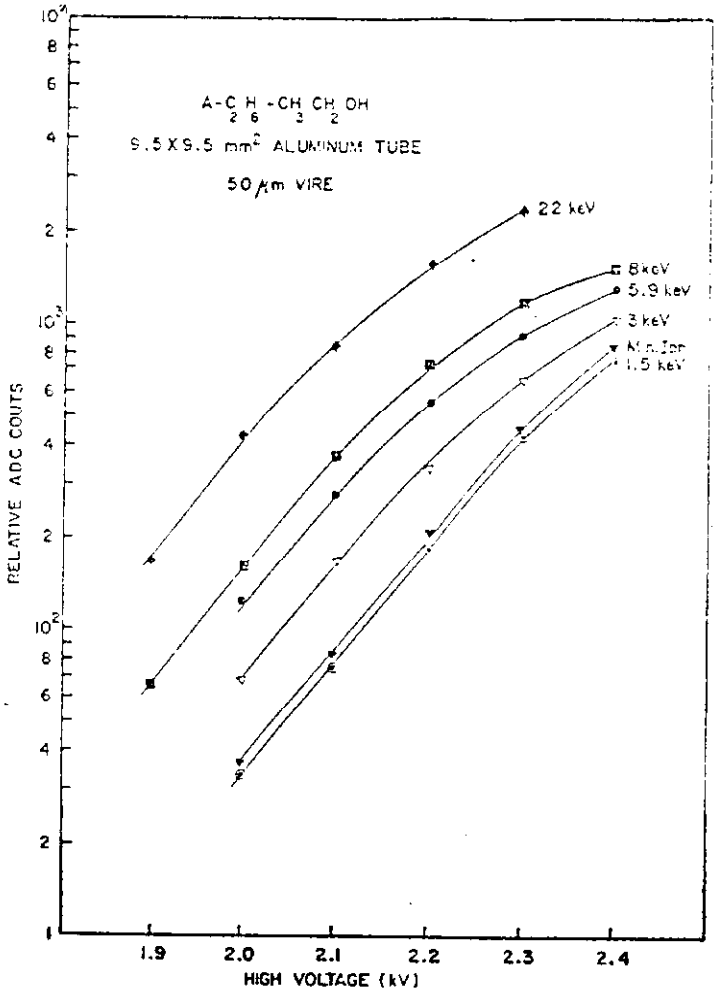

Fig. 5

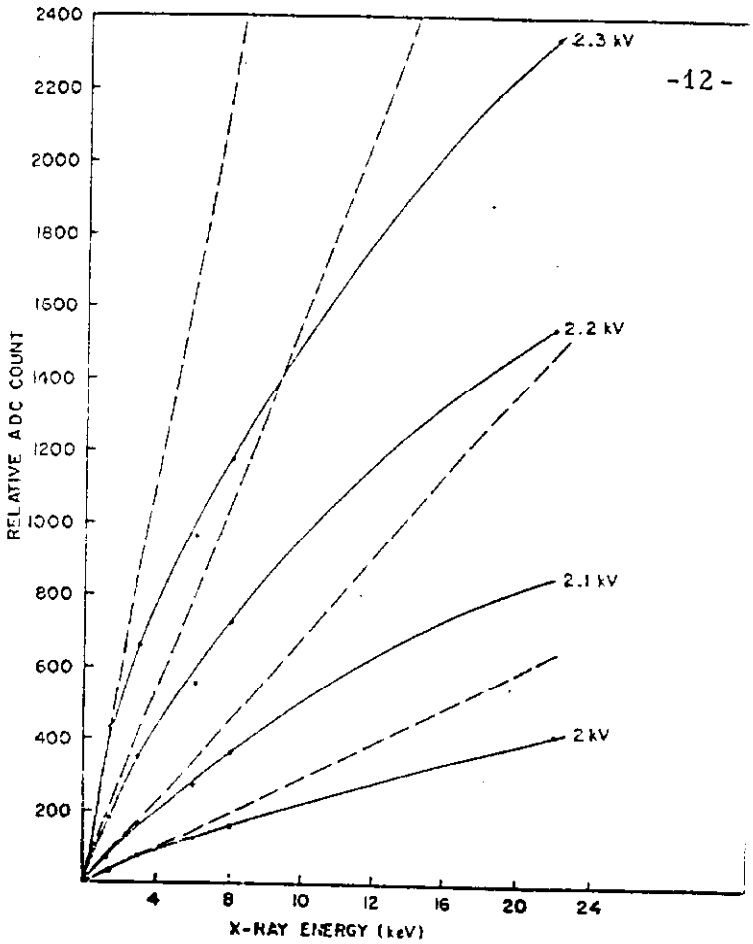

Fig. 6

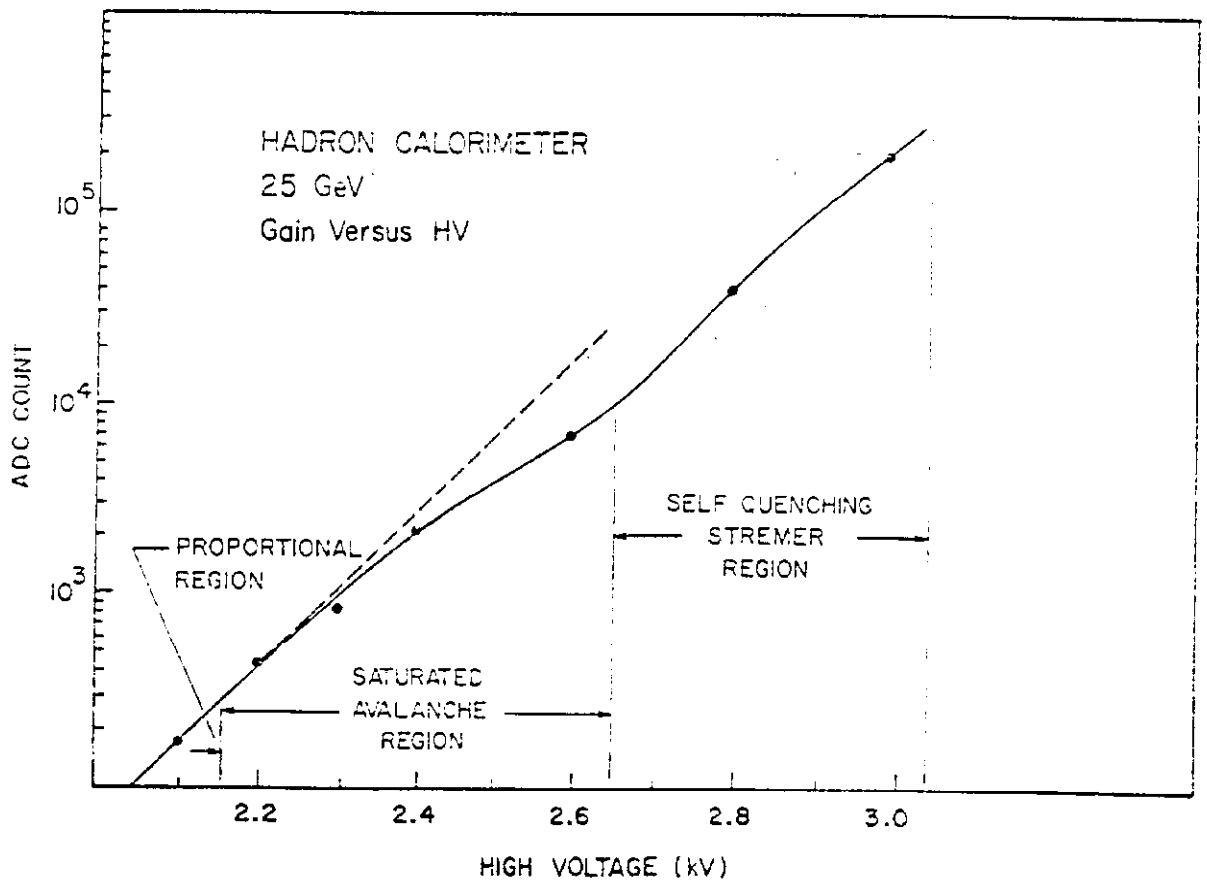

Fig. 7

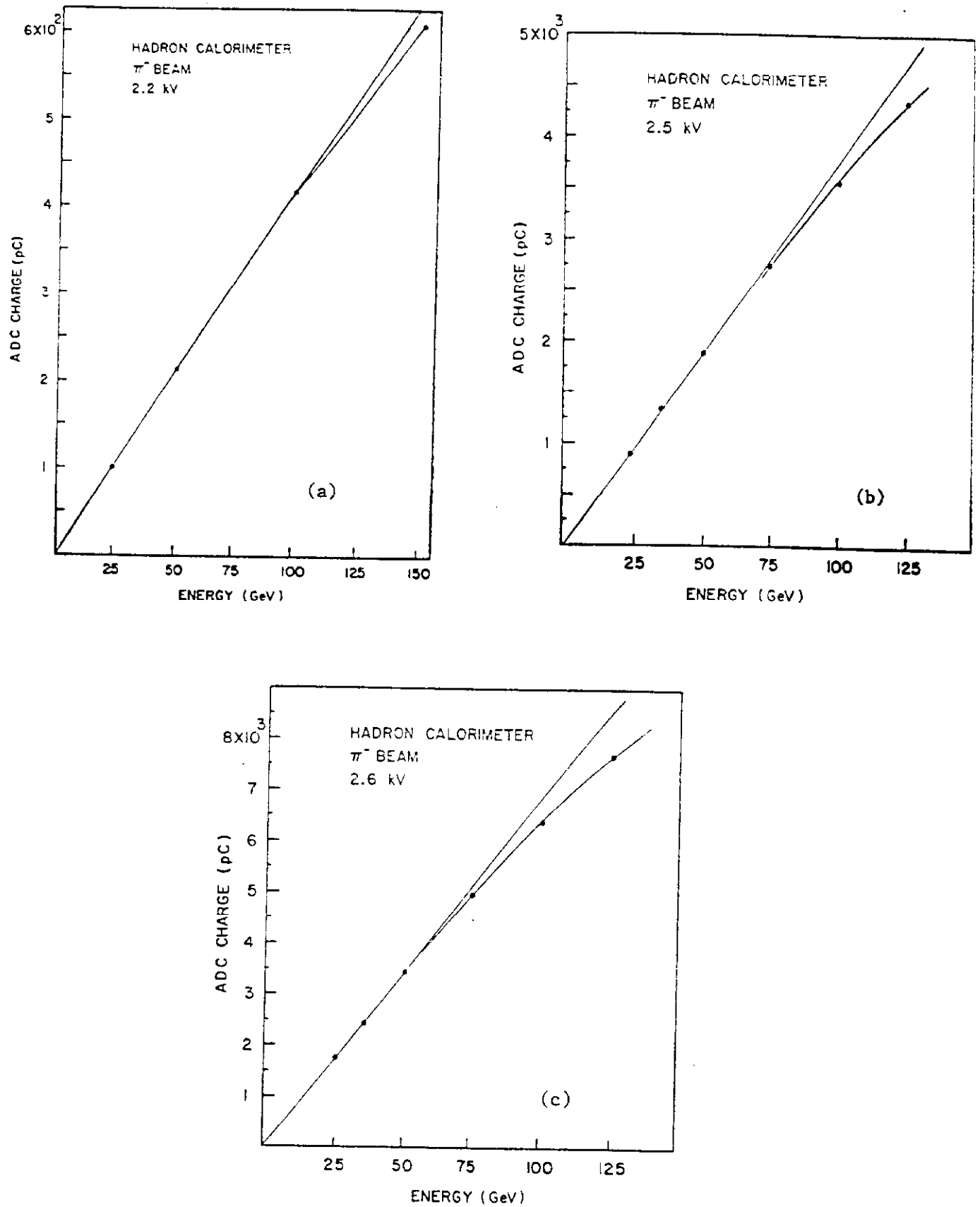
6X10^2
HADRON CALORIMETER
π⁻ BEAM
2.2 kV
ADC CHARGE (pC)
ENERGY (GeV)
(a)
5X10^3
HADRON CALORIMETER
π⁻ BEAM
2.5 kV
ADC CHARGE (pC)
ENERGY (GeV)
(b)
8X10^3
HADRON CALORIMETER
π⁻ BEAM
2.6 kV
ADC CHARGE (pC)
ENERGY (GeV)
(c)

Fig. 8

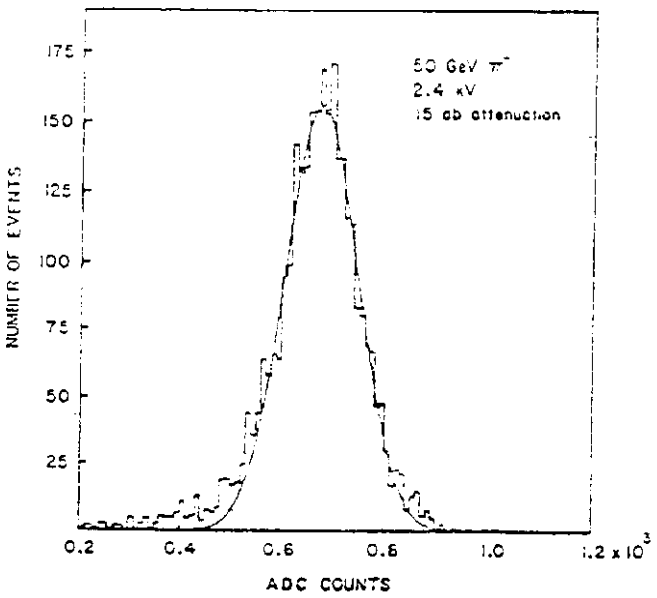

Fig. 9a

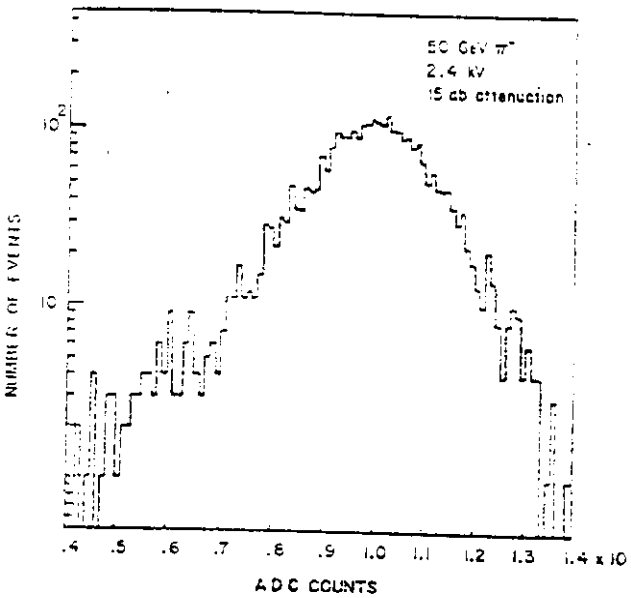

Fig. 9b

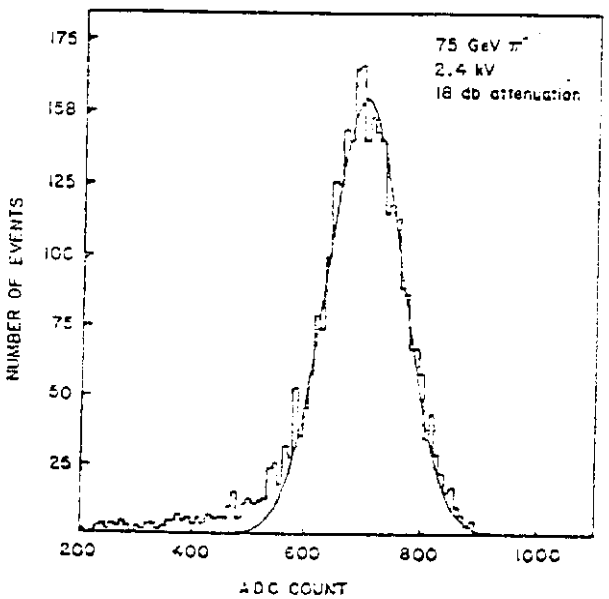

Fig. 10a

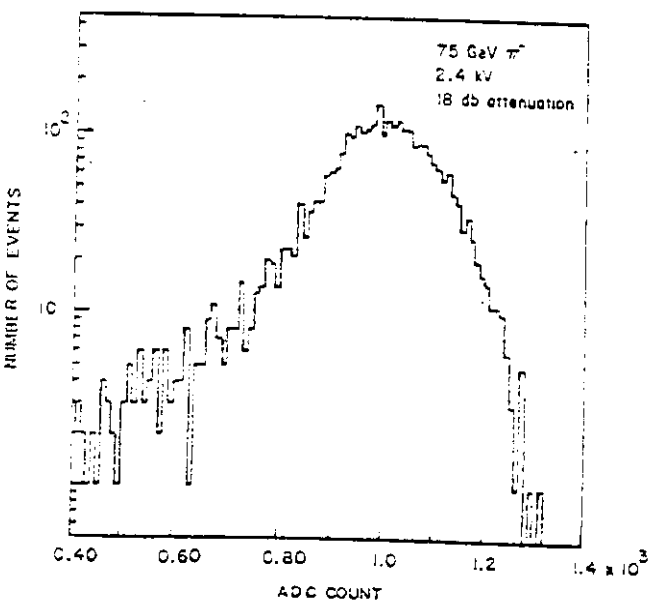

Fig. 10b

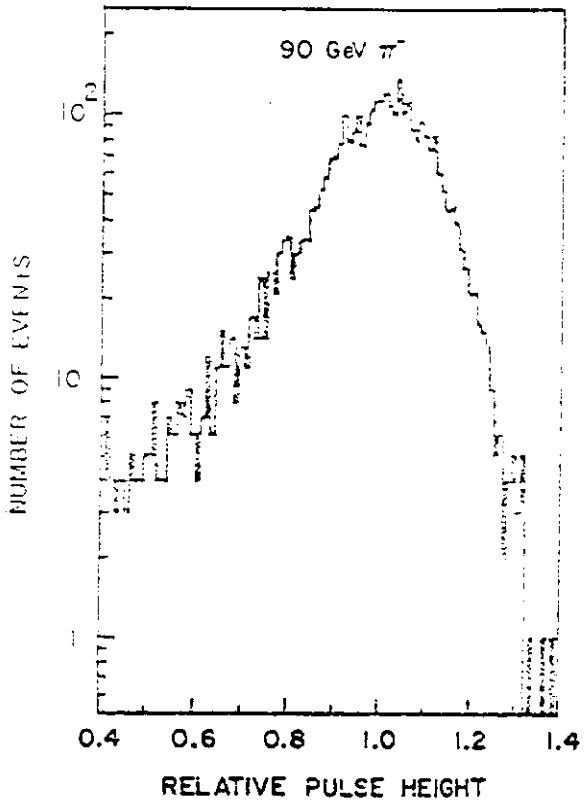

Fig. 11

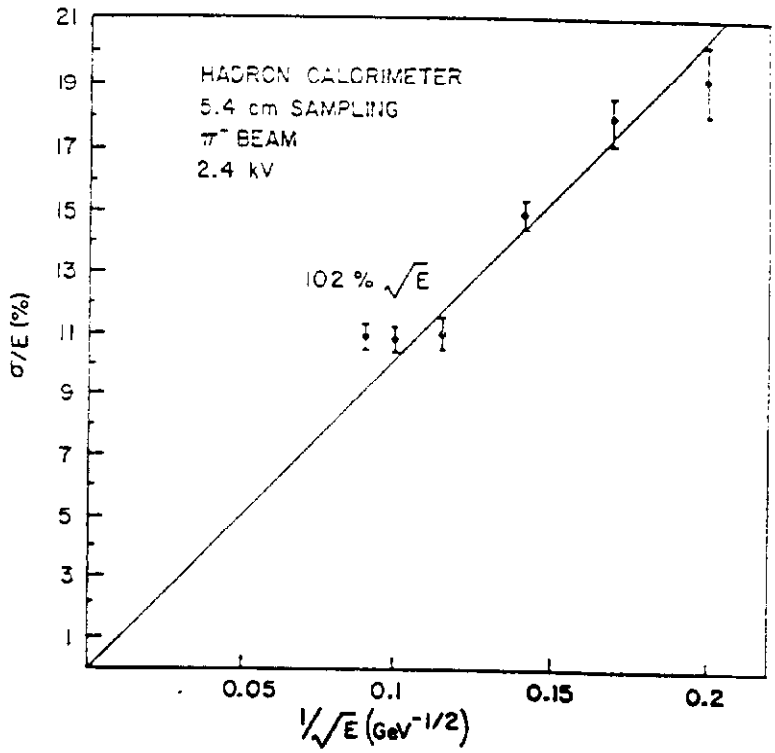

Fig. 12

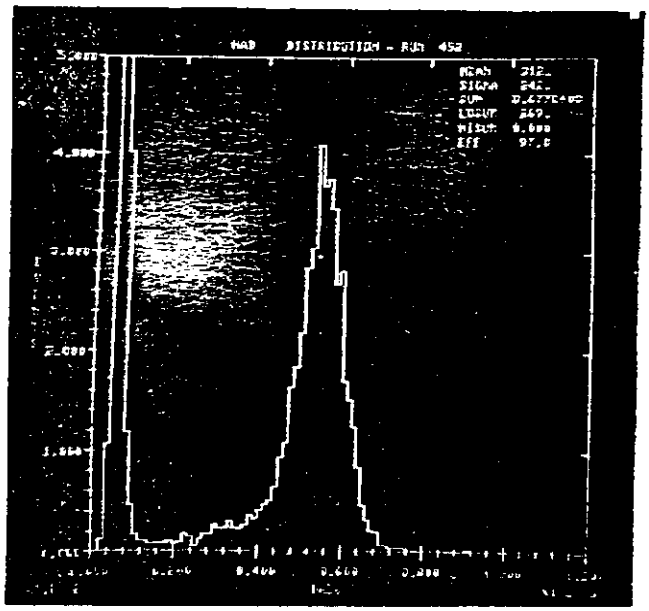

Fig. 13a

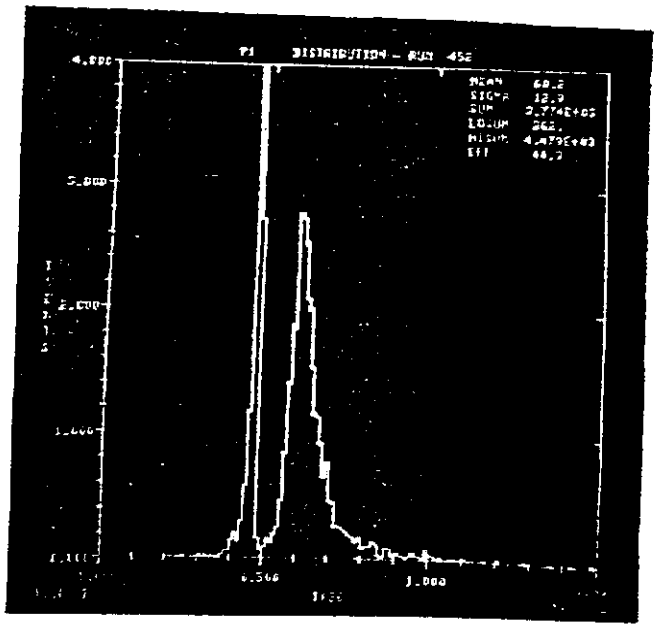

Fig. 13b

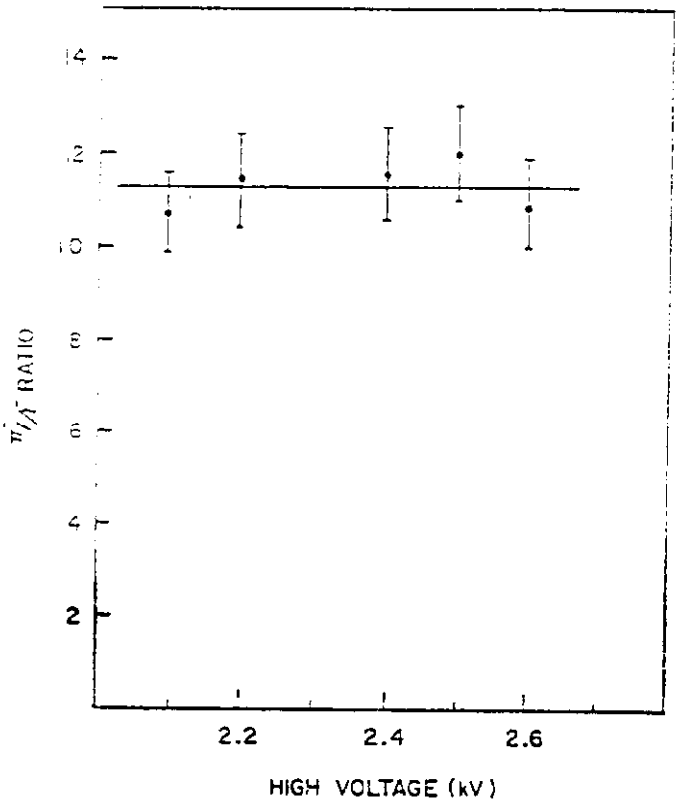
π/λ^- RATIO
14
12
10
8
6
4
2
2.2
2.4
2.6
HIGH VOLTAGE (kV)

Fig. 14

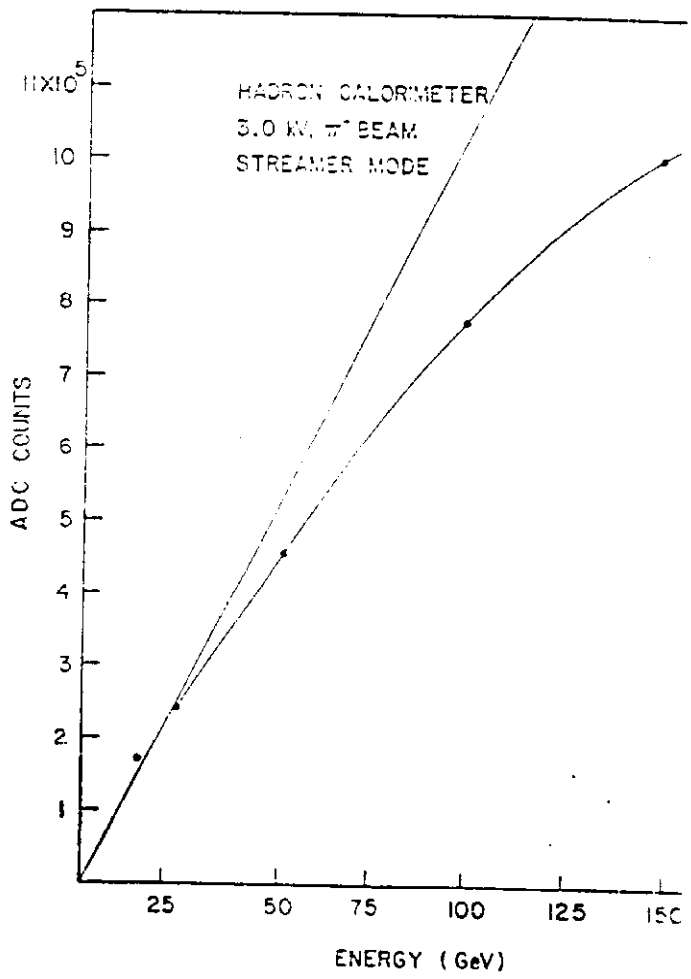
HADRON CALORIMETER
3.0 kV, π^- BEAM
STREAMER MODE
ADC COUNTS
11X10^5
10
9
8
7
6
5
4
3
2
1
25
50
75
100
125
150
ENERGY (GeV)

Fig. 15

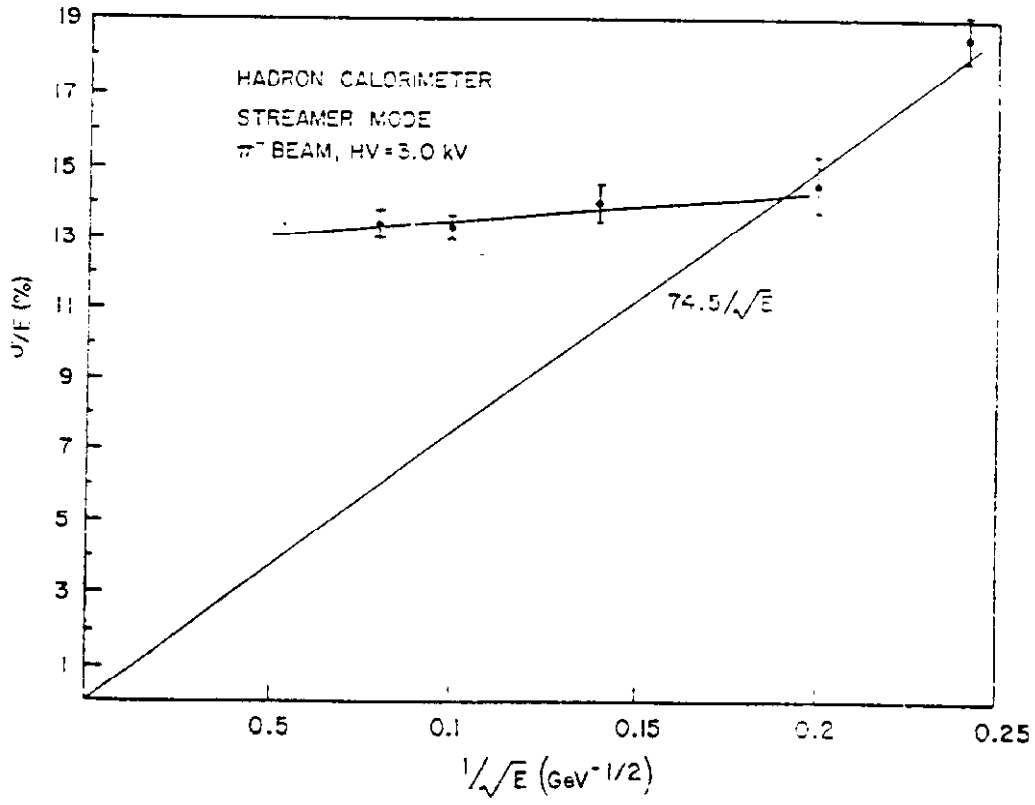
HADRON CALORIMETER
STREAMER MODE
π^- BEAM, HV = 3.0 kV
$74.5/\sqrt{E}$
σ/E (%)
19
17
15
13
11
9
7
5
3
1
0.5
0.1
0.15
0.2
0.25
$1/\sqrt{E}$ (GeV$^{-1/2}$)

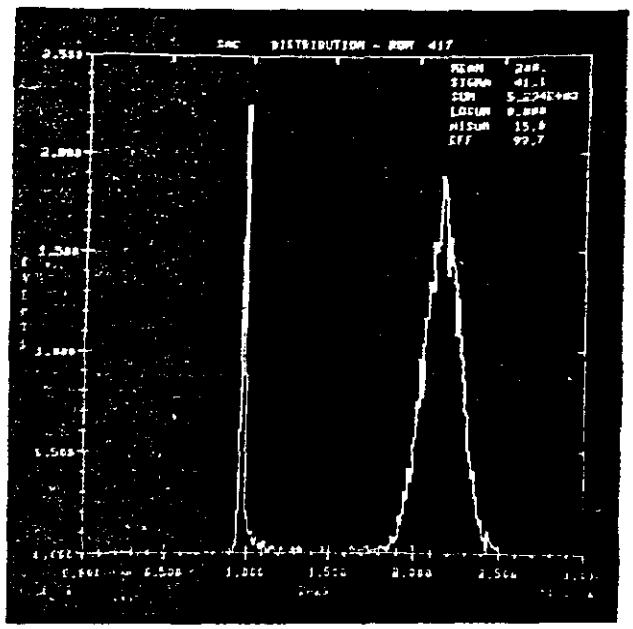

Fig. 17

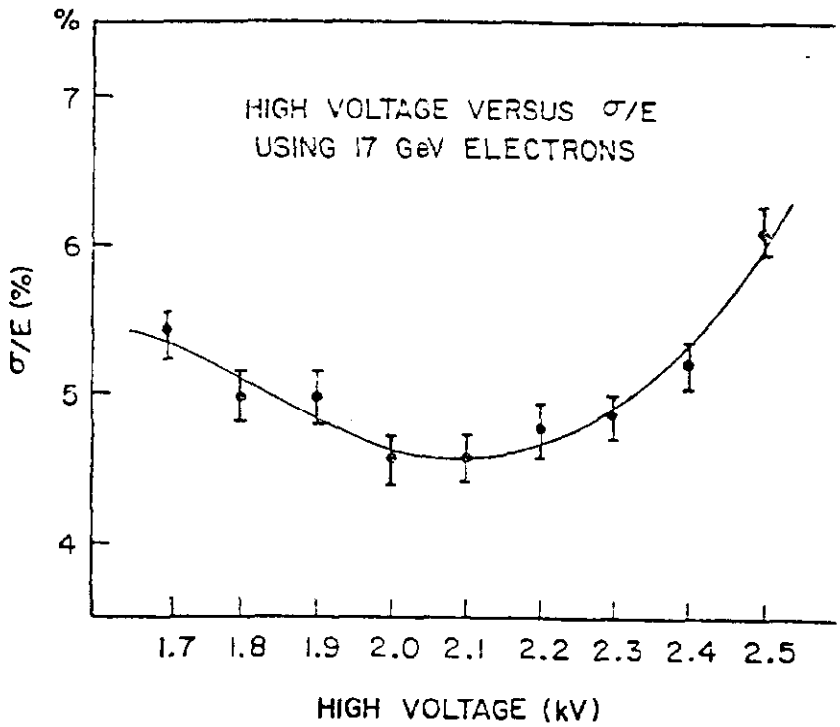

Fig. 18

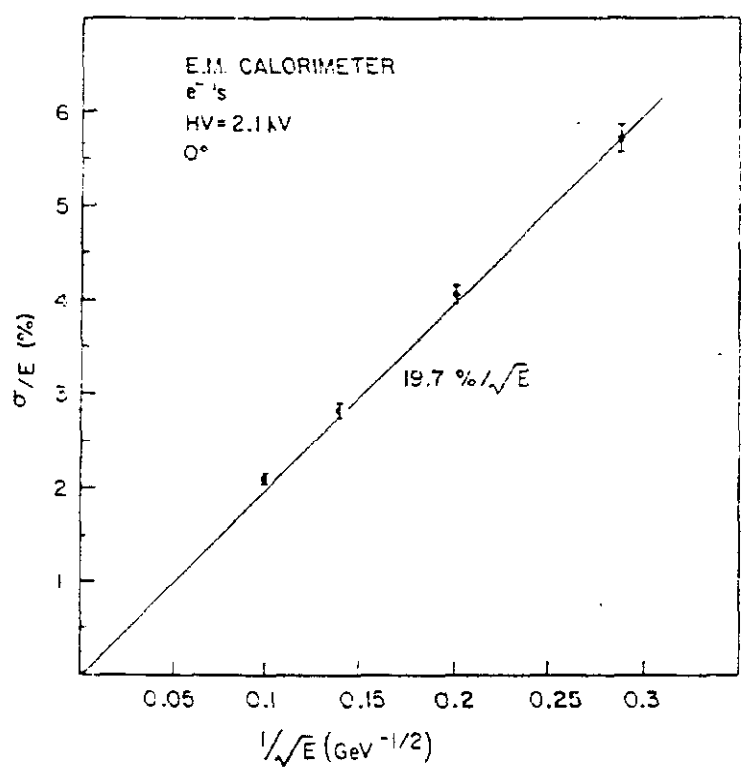

Fig. 19

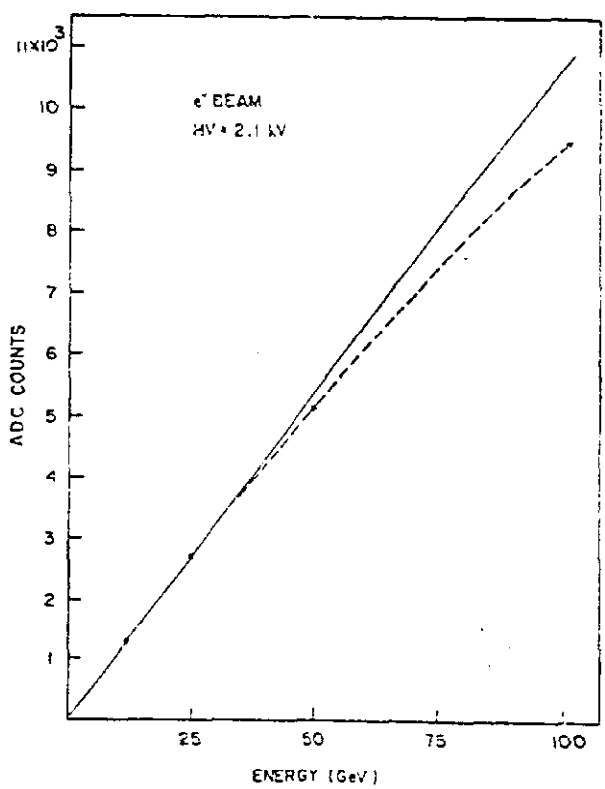

Fig. 20